PROCEEDINGS OF SCIENCE

posurl[1]

Evidence for triboson ZZγ production in the $4l\gamma$ final state in pp collisions at 13 TeV with the CMS experiment

Antonio Vagnerini[a,1,*]

[a] *University of Lincoln-Nebraska,*
1400 R St, Lincoln, NE 68588, US

E-mail: antonio.vagnerini@cern.ch

We present the first measurement of ZZγ production in the final state with four charged leptons and a photon using the full LHC Run 2 data set. This analysis uses the proton-proton collision data at a center-of-mass energy of 13 TeV collected by the CMS detector from 2016 to 2018 with a total integrated luminosity of 138 fb^{-1}. The first evidence for the triboson process pp $\rightarrow ZZ\gamma \rightarrow 4\ell\gamma$ is reported, with the observed (expected) significance found to be 3.7 (3.0) standard deviations. The corresponding measured (expected) fiducial cross section is 56^{+34}_{-28} ab (48 ± 23 ab). Furthermore, an additional measurement is performed by including the initial and final state radiation component in the signal definition. In this case, an observed (expected) significance of 5.1 (4.1) standard deviations is found for the electroweak production of pp $\rightarrow 4\ell\gamma$, and the corresponding measured (expected) fiducial cross section of 162^{+66}_{-58} ab (100 ± 31 ab). Both measurements are in agreement with the Standard Model predictions at the level of one standard deviation.

2025 European Physical Society Conference on High Energy Physics (EPS-HEP2025)
7–11th July 2025
Marseille, France

[1]on behalf of the CMS Collaboration
*Speaker

PoS(EPS-HEP2025)280

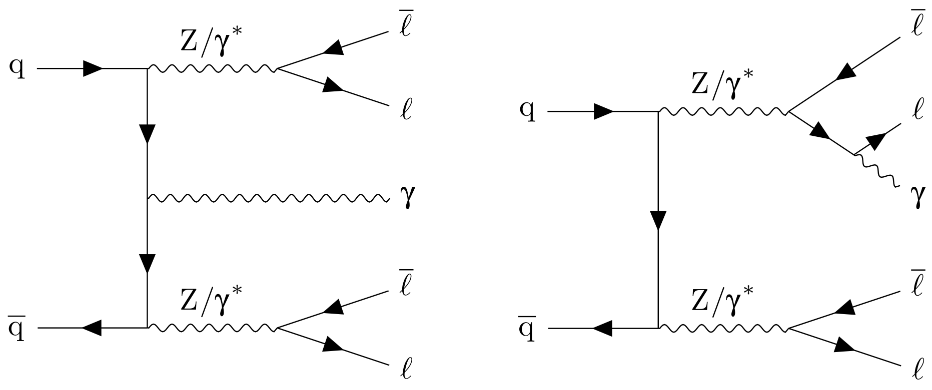

Figure 1: Representative tree-level Feynman diagrams with four isolated leptons and a photon in the final state in the Standard Model.

The production of three electroweak bosons is extremely rare at the LHC, with cross sections of the order of tens of femtobarns. Triboson processes include contributions from triple and quartic gauge couplings at tree level, as well as diagrams mediated by the Higgs boson. Their measurement allows setting stringent constraints on the electroweak sector at a higher scale than the Higgs boson mass. The ATLAS [1, 2] and CMS [3] Collaborations have reported the observation of photon pair production with a massive vector boson V at 13 TeV, and also observed the WZγ process [4, 5]. The CMS experiment [6] has reported the observation of WWγ production [7], while the triple VVV production has been observed by both ATLAS [8] and CMS [9]. An extensive review on the triboson processes can be found in Refs. [10, 11].

The production of a Z boson pair and a photon (ZZγ) is the rarest triboson process, since the SM gauge symmetry forbids the presence of tri- and quadri-linear neutral gauge bosons couplings at tree-level. The ZZγ and ZZ$\gamma\gamma$ vertices can only be generated at loop-level, typically via fermion triangle diagrams. These processes can be enhanced in extended gauge sectors and studied using higher-dimensional operators in dimension-8 Effective Field Theories (EFTs). In the electroweak production of two lepton pairs and a photon, the latter may originate from the initial-state radiation (ISR) emitted from a quark, or from the final state radiation (FSR) from a charged lepton, as exemplified in Fig. 1. The associated production of a Higgs boson with a Z boson, followed by the rare decay ZH(H→Zγ), provides a minor contribution to the ZZγ production, around 5%.

In this analysis, a search for pp →ZZγ with both Z bosons decaying leptonically [13] is done using proton-proton collision data collected by the CMS detector [12] at $\sqrt{s}$ = 13 TeV during LHC Run 2, with 138 fb^{-1} of integrated luminosity. In addition, an inclusive search region is employed to incorporate both ISR and FSR as part of the signal definition. The final state consists of two pairs of oppositely-charged leptons, i.e. electrons or muons, and a photon.

The inclusive signal process $pp \rightarrow 4l\gamma$ is modeled at next-to-leading order (NLO) in QCD and leading order (LO) in EW interactions. This sample includes the triboson process $ZZ\gamma \rightarrow 4l\gamma$ of interest, the non-resonant diagrams with $Z^*/\gamma^* \rightarrow l^+l^-$, and the contribution from final state radiation. The rare $ZH \rightarrow Z(H \rightarrow Z\gamma)$ signal process and the main backgrounds $(q\bar{q}/qg) \rightarrow ZZ \rightarrow 4l$ are also estimated from simulation. To prevent the double counting of FSR photons, events with prompt photons at generator level passing the fiducial selection of the inclusive $pp \rightarrow 4l\gamma$

region are removed from the main background samples. Other rare backgrounds include the triple massive vector boson VVV (V = Z, W), $t\bar{t}$, as well as $t\bar{t}+V$, and $t\bar{t}+VV = \{WW/ZZ\}$ production.

The kinematic selection on the charged leptons is designed to match the detector acceptance. This includes a transverse momentum threshold of $p_T^{e,(\mu)} > 7$ (5) GeV, and a pseudorapidity window of $|\eta^{e,(\mu)}| < 2.5$ (2.4). To ensure that leptons are isolated, the scalar sum of the transverse momenta of particles within a cone of radius $\Delta R = \sqrt{\Delta\eta^2 + \Delta\phi^2} = 0.3$ around the lepton momentum direction is required to be less than $0.35\, p_T^l$. To improve the Z boson mass reconstruction, FSR photons stemming from Z boson decays are recovered with the following algorithm. Photons satisfying $|\eta^\gamma| < 2.4$, $p_T^\gamma > 20$ GeV, and a relative isolation $I_\gamma < 1.8$ are considered as FSR candidates, excluding those already employed in the electron reconstruction. FSR photons typically have a harder energy spectrum than those from pileup interactions and are expected to be quasi-collinear with the emitting leptons. Therefore each FSR candidate is paired with the nearest lepton under the condition that $\Delta R(l,\gamma)/(p_T^\gamma)^2 > 0.012$ GeV^{-2} and $\Delta R(\gamma, l) < 0.5$. For each lepton, the FSR candidate with the lowest value of $\Delta R(\gamma, l)/(p_T^\gamma)^2$, if any, is selected and its four-momentum is added to that of the associated lepton.

Signal photon candidates with $p_T^\gamma > 20$ GeV and $|\eta^\gamma| < 1.444$ or $1.566 < |\eta^\gamma| < 2.4$, must be well-separated from any final state lepton by $\Delta R(l,\gamma) > 0.5$ and are identified using a cut-based discriminant and a multivariate one [15]. The former is based upon the electromagnetic shower-shape variables, the energy deposition in the electromagnetic calorimeter, and the photon relative isolation from charged hadrons, neutral ones and other photons. A working point with an average selection efficiency of genuine photons of approximately 90% is used to define tight photons. Loose photons may fail the shower-shape or the charged-hadron isolation criteria, while still satisfying the remaining ones. In contrast, the multivariate discriminant employs fourteen input features, and only a tight working point is defined, corresponding to an average selection efficiency of 80%.

Events are initially selected using a combination of multi-lepton triggers [14] with either two loosely isolated leptons, three low-p_T leptons or a single charged lepton. Each event must contain two Z boson candidates reconstructed from a pair of isolated leptons with the same flavor and opposite charge. Both Z candidates must have an invariant mass between 60 and 120 GeV. The Z candidate whose mass is closest to 91.2 GeV is denoted Z_1, while the other is referred to as Z_2. The (sub) leading lepton must satisfy $p_T > 20(10)$ GeV. Every lepton must be spatially separated from all others by $\Delta R(l_i, l_j) > 0.02$. Events containing pairs of oppositely charged leptons whose invariant mass $m_{l^+l'^-}$ is less than 4 GeV are rejected, regardless of flavor, to suppress low-mass resonances. In addition, events with four electrons (muons) are discarded if the same four leptons can alternatively stem from two Z bosons, Z_a and Z_b, such that $m_{Z_b} < 12$ GeV and m_{Z_a} is closer to 91.2 GeV than the original Z_1. This criterion suppresses events containing an on-shell Z boson in association with a low-mass resonance. In the triboson signal region, an additional requirement is imposed: the lowest invariant mass of each lepton pair and the photon, $\min(m_{ll\gamma}, m_{l'l'\gamma})$, must exceed 100 GeV to suppress the FSR contamination.

Several photon identification methods have been explored to estimate the non-prompt photon contamination for the inclusive $pp \to l^+l^-l'^+l'^-\gamma$ region and the triboson $pp \to ZZ\gamma \to 4l\gamma$ one. The cut-based identifier is adopted for the inclusive one since a control region with sufficient statistics for the data-driven background estimation can be defined. The multivariate photon discriminant is instead used in the triboson region to suppress the non-prompt photon background from simulation.

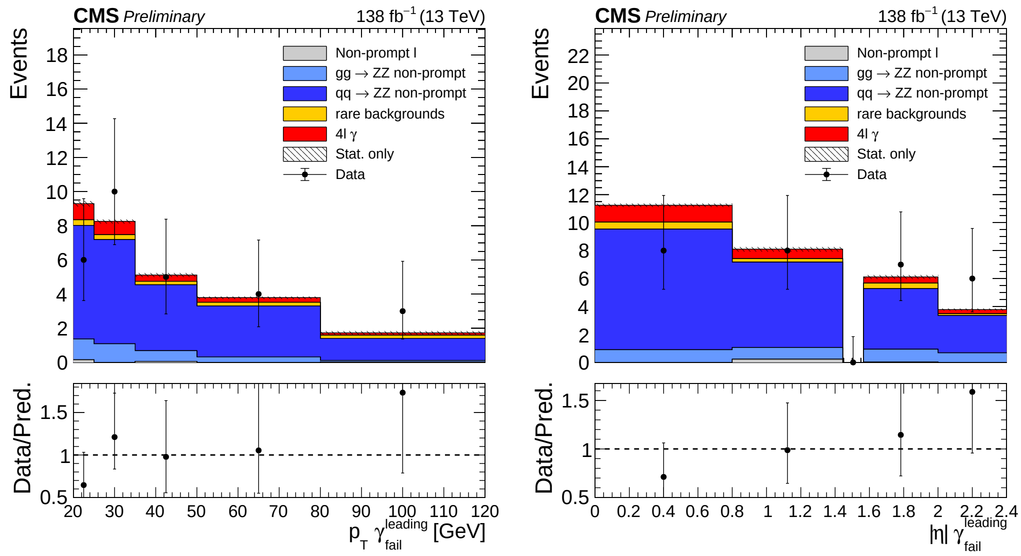

Figure 2: Transverse momentum (left) and pseudorapidity (right) of the leading photon passing the *loose* selection and failing the *tight* cut-based selection in the non-prompt photon application region with four leptons passing the tight selection [13].

Dedicated control regions are defined to estimate the non-prompt lepton and non-prompt photon backgrounds, while other rare backgrounds are estimated from simulation. Non-prompt leptons originate from processes in which at least one final state lepton does not come from the decay of a W or Z boson. The main sources are the decays of heavy-flavor mesons producing non-isolated leptons, as well as light-flavor jets and electrons from photon conversions. This small background is estimated using the method employed in the search for $H \to$ ZZ decays described in Ref. [16].

Non-prompt photons constitute the main instrumental background arising from either highly-energetic light-flavor jets, which often contain photons from light-mesons decays, or from misidentified electrons. A tight-to-loose method is employed to estimate this background with a data-driven approach in the inclusive region. The photon misidentification rate, i.e. the probability for a non-prompt photon passing the loose identification to satisfy the tight selection, is obtained in a control region after the subtraction of the Z$\to\gamma$ contributions from simulation. The application region differs from the signal region by the requirement that the photon must fail the tight selection. Figure 2 illustrates the good level of data-to-simulation agreement in the non-prompt photon estimation. The corresponding yield in the signal region is inferred by reweighting the events in the application region with the misidentification rate.

The cross section measurements are extracted using a maximum-likelihood template fit of the expected signal and background distributions of the main observable $m_{4l\gamma}$ to the observed data. The fit includes a single parameter of interest, i.e. the signal strength, defined as the ratio of the measured fiducial cross section to the expected SM prediction. The significance for which the background-only hypothesis is disfavored is determined as the integral of the appropriate test statistic distribution using the asymptotic approximation [17]. A fiducial region where the contribution from the final state radiation is highly suppressed is used, consisting of the following kinematic photon selection: $p_T^\gamma > 20\,\text{GeV}$, $|\eta^\gamma| < 2.4$, $\Delta R(\ell,\gamma) > 0.5$, for the inclusive region. In addition the

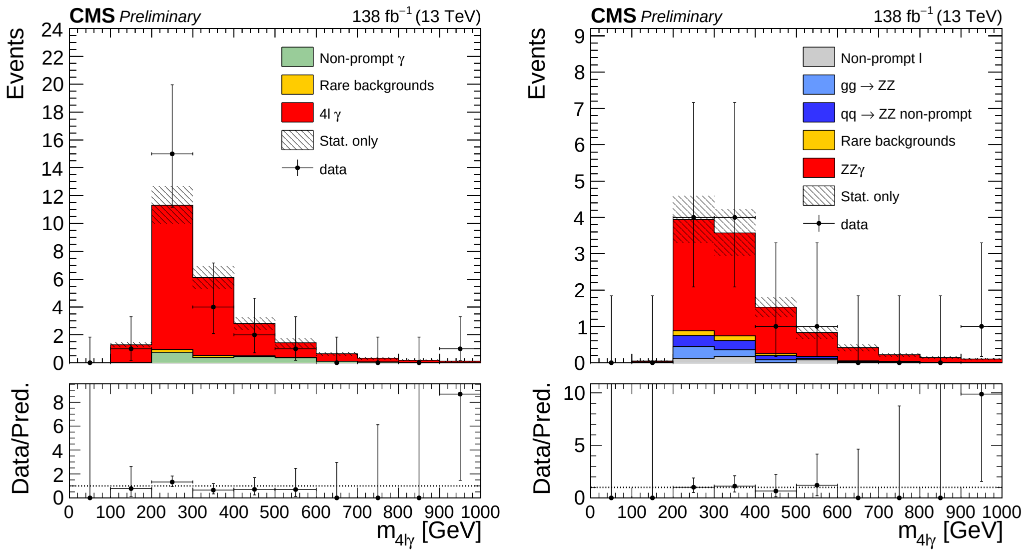

Figure 3: Invariant mass spectra of the four-lepton-plus-photon system in the inclusive $pp \rightarrow l^+l^-l'^+l'^-\gamma$ (left) and triboson ZZγ (right) regions, with the cut-based and MVA photon identification, respectively [13].

$\min(m_{Z\gamma}) > 100$ GeV requirement is applied for the triboson-specific region.

In the inclusive $pp \rightarrow l^+l^-l'^+l'^-\gamma$ region, the statistical uncertainty dominates, accounting for over 90% of the overall uncertainty. The leading systematic uncertainties arise from the QCD scale (5% impact), the electron efficiency (4%), and the shape and normalization of the non-prompt photon background (4%). The corresponding fiducial cross section is determined to be $\sigma_{\text{fid}}(pp \rightarrow 4l\gamma) = 162^{+64}_{-56}(\text{stat})^{+7}_{-9}(\text{theo})^{+5}_{-4}(\text{lumi})^{+15}_{-14}(\text{syst})\,\text{ab} = 162^{+66}_{-58}$ ab.

The observed (expected) significance of the signal relative to the background-only hypothesis is 5.1 (4.1) standard deviations. In the triboson region, the statistical uncertainty also dominates, accounting for over 98% of the total uncertainty. The dominant systematic uncertainties affect the normalization of the $q\bar{q} \rightarrow ZZ$ non-prompt background with an impact of 4% on the signal strength and the electron efficiency (4%). In this case, the fiducial cross section is $\sigma_{\text{fid}}(pp \rightarrow ZZ\gamma \rightarrow 4l\gamma) = 56^{+34}_{-28}(\text{stat})^{+1}_{-1}(\text{theo})^{+2}_{-1}(\text{lumi})^{+6}_{-5}(\text{syst})\,\text{ab} = 56^{+34}_{-28}$ ab. The observed (expected) significance of ZZγ triboson production is found to be 3.7 (3.0) standard deviations. In summary, this measurement provides the first evidence for the triboson process, $pp \rightarrow$ ZZγ, where each Z boson decays leptonically to electrons or muons.

References

[1] ATLAS Collaboration, "Measurement of $Z\gamma\gamma$ production in pp collisions at $\sqrt{s} = 13$ TeV with the ATLAS detector", EPJC 83, 539 (2023), [arXiv:2211.14171]

[2] ATLAS Collaboration, "Observation of $W\gamma\gamma$ triboson production in proton-proton collisions at $\sqrt{s} = 13$ TeV with the ATLAS detector", Phys. Lett. B848, 138400 (2024), [arXiv:2308.03041]

[3] CMS Collaboration, "Measurements of the $pp \to W^{\pm}\gamma\gamma$ and $pp \to Z\gamma\gamma$ cross sections at $\sqrt{s}$ = 13 TeV and limits on anomalous quartic gauge couplings", JHEP 10, 174 (2021), [arXiv:2105.12780]

[4] ATLAS Collaboration, "Observation of $WZ\gamma$ production in pp collisions at $\sqrt{s}$ = 13 TeV with the ATLAS Detector", Phys. Rev. Lett. 132, 021802 (2024), [arXiv:2305.16994]

[5] CMS Collaboration, "Observation of $WZ\gamma$ production and constraints on new physics scenarios in proton-proton collisions at $\sqrt{s}$ = 13 TeV", Phys. Rev. D112, 012009 (2025), [arXiv:2503.21977]

[6] CMS Collaboration, "The CMS experiment at the CERN LHC", JINST 3 (2008) S08004, doi:10.1088/1748-0221/3/08/S08004

[7] CMS Collaboration, "Observation of WWγ production and search for Hγ production in proton-proton collisions at $\sqrt{s}$ = 13 TeV", Phys. Rev. Lett. 132, 121901 (2024), [arXiv:2310.05164]

[8] ATLAS Collaboration, "Evidence for the production of three massive vector bosons with the ATLAS detector", Phys. Lett. B798, 134913 (2019), [arXiv:1903.10415]

[9] CMS Collaboration, "Observation of the production of three massive gauge bosons at $\sqrt{s}$ = 13 TeV", Phys. Rev. Lett. 125, 151802 (2020), [arXiv:2006.11191]

[10] ATLAS Collaboration, "Exploration at the high-energy frontier: ATLAS Run 2 searches investigating the exotic jungle beyond the Standard Model", Phys. Rep., 2024, [arXiv:2403.09292]

[11] CMS Collaboration, "Stairway to discovery: a report on the CMS programme of cross section measurements from millibarns to femtobarns", Phys. Rept. 1115 (2025) 3, [arXiv:2405.18661]

[12] CMS Collaboration, "Development of the CMS detector for the CERN LHC Run 3", JINST 19 (2024) P05064, doi:10.1088/1748-0221/19/05/P05064

[13] CMS Collaboration, "Observation of 4$l\gamma$ and evidence of $ZZ\gamma$ production in proton-proton collisions at $\sqrt{s}$ = 13 TeV", CMS-PAS-SMP-24-014, [https://cds.cern.ch/record/2932923]

[14] CMS Collaboration, "The CMS trigger system", JINST 12, P01020 (2017), [arXiv:1609.02366]

[15] CMS Collaboration, "Electron and photon reconstruction and identification with the CMS experiment at the CERN LHC", JINST 16, P05014 (2021), [arXiv:2012.06888]

[16] CMS Collaboration, "Measurement of the properties of a Higgs boson in the four-lepton final state", Phys. Rev. D89, 092007 (2014), [arXiv:1312.5353]

[17] G. Cowan, K. Cranmer, E. Gross, O. Vitells, "Asymptotic formulae for likelihood-based tests of new physics", Eur. Phys. J. C71, 1554 (2011), [arXiv:1007.1727]

PoS(EPS-HEP2025)280